



# Deep learning–based downscaling of summer monsoon rainfall data over Indian region

Bipin Kumar<sup>1</sup> · Rajib Chattopadhyay<sup>1</sup> · Manmeet Singh<sup>1,2</sup> · Niraj Chaudhari<sup>3</sup> · Karthik Kodari<sup>4</sup> · Amit Barve<sup>3</sup>

Received: 30 October 2020 / Accepted: 25 November 2020 / Published online: 2 January 2021

© The Author(s), under exclusive licence to Springer-Verlag GmbH, AT part of Springer Nature 2021

## Abstract

Downscaling is necessary to generate high-resolution observation data to validate the climate model forecast or monitor rainfall at the micro-regional level operationally. Available observations generated by automated weather stations or meteorological observatories are often limited in spatial resolution resulting in misrepresentation or absence of rainfall information at these levels. Dynamical and statistical downscaling models are often used to get information at high-resolution gridded data over larger domains. As rainfall variability is dependent on the complex spatio-temporal process leading to non-linear or chaotic spatio-temporal variations, no single downscaling method can be considered efficient enough. In the domains dominated by complex topographies, quasi-periodicities, and non-linearities, deep learning (DL)–based methods provide an efficient solution in downscaling rainfall data for regional climate forecasting and real-time rainfall observation data at high spatial resolutions. We employed three deep learning-based algorithms derived from the super-resolution convolutional neural network (SRCNN) methods in this work. Summer monsoon season data from India Meteorological Department (IMD) and the tropical rainfall measuring mission (TRMM) data set were downscaled up to 4 times higher resolution using these methods. High-resolution data derived from deep learning-based models provide better results than linear interpolation for up to 4 times higher resolution. Among the three algorithms, namely, SRCNN, stacked SRCNN, and DeepSD, employed here, the best spatial distribution of rainfall amplitude and minimum root-mean-square error is produced by DeepSD-based downscaling. Hence, the use of the DeepSD algorithm is advocated for future use. We found that spatial discontinuity in amplitude and intensity rainfall patterns is the main obstacle in the downscaling of precipitation. Furthermore, we applied these methods for model data post-processing, in particular, ERA5 reanalysis data. Downscaled ERA5 rainfall data show a much better distribution of spatial covariance and temporal variance when compared with observation. This study is the first step towards developing deep learning-based weather data downscaling model for Indian summer monsoon rainfall data.

**Keywords** Deep learning method · Statistical downscaling · Super-resolution · Rainfall data over Indian region

## 1 Introduction

Downscaling of rainfall data over Indian region during the summer monsoon season is difficult as the summer monsoon rainfall results from a multi-scale spatio-temporal dynamical process with significant variance (Chang et al. 2018). It is a complex interacting system with various climate teleconnections playing a considerable role in rainfall variabilities such as ENSO (Sikka 1980; Pant and Parthasarathy 1981), PDO (Krishnan and Sugi 2003), IOD (Ashok et al. 2001), and volcano (Singh et al. 2020). Hence, regional variations of monsoon rainfall are often quite large varying from a few millimeters to thousands of millimeters within a few hundred kilometers (e.g., near the Western Ghats) and over several belts of the Himalayas. Figure 1a and b show the high

---

✉ Bipin Kumar  
bipink@tropmet.res.in

<sup>1</sup> Indian Institute of Tropical Meteorology, Ministry of Earth Sciences, Dr. Homi Bhabha Road, Pashan 411008, India

<sup>2</sup> IDP in Climate Studies, Indian Institute of Technology Bombay, Mumbai, India

<sup>3</sup> Ramrao Adik Institute of Technology, Nerul, Navi Mumbai, MH 400706, India

<sup>4</sup> Defence Institute of Advanced Technology, Girinagar, Pune, MH 411025, India

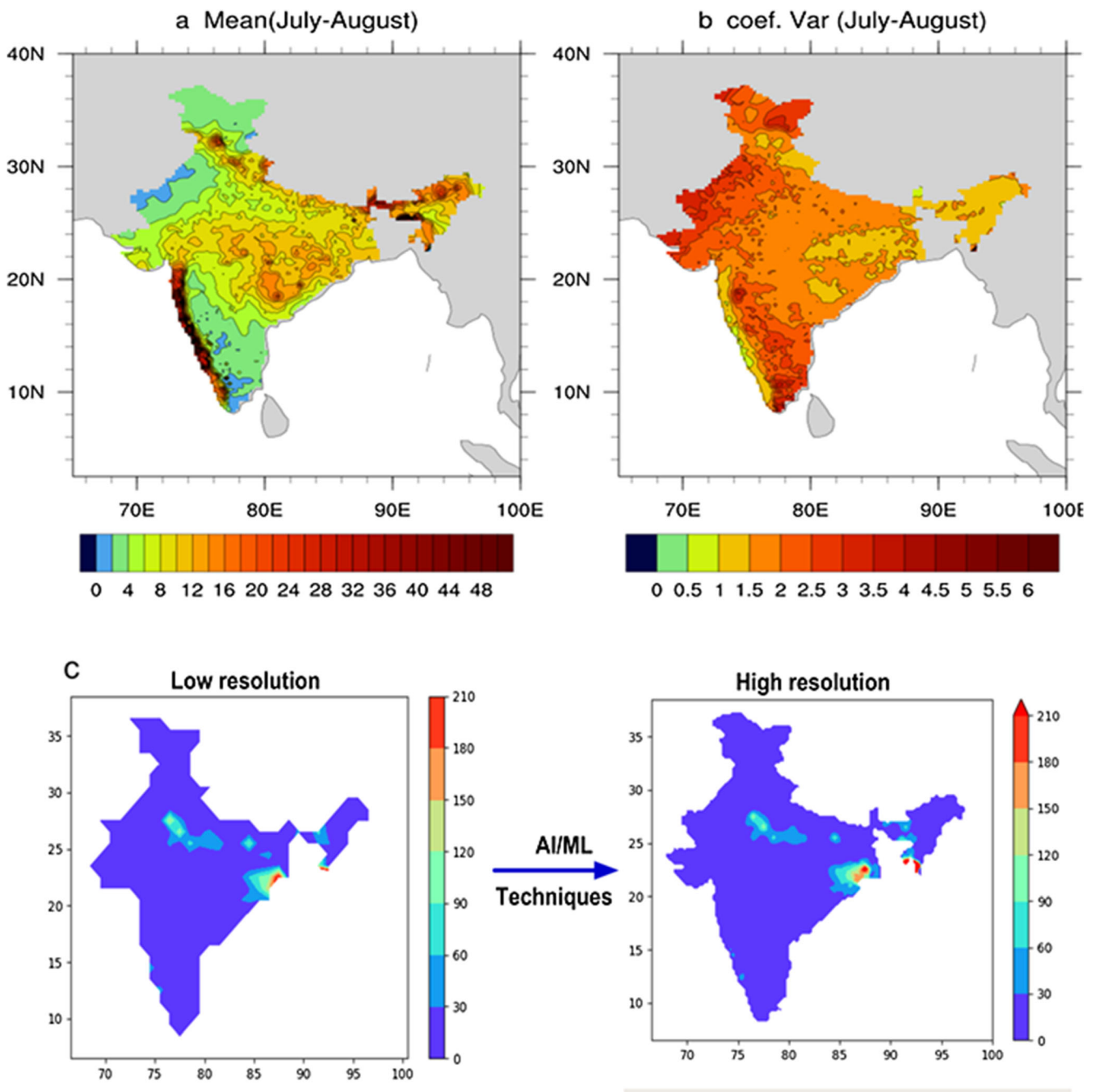


**Fig. 1** Upper panel plots showing the July–August mean rainfall millimeters per day (**a**) and coefficient of variation (CoV) (**b**) for the years 1981–2010. The region with low mean has high dispersion and high mean has low dispersion. It is clear from these panels that there are sharp

spatial gradients of CoV along the orographic variation zones, especially in the Western Ghats and northern Himalayan belts. Lower panel plot (**c**) illustrates the concept of downscaling of rainfall data. These units of rainfall in legends are millimeter/day

degree of spatial dispersion and spatial gradient in the distribution along the Western Ghats region and high gradient in the monthly averaged rainfall. Monsoon rainfall can be classified into several coherently fluctuating zones, which may be linked to complex multi-scale processes (Gadgil et al. 1993; Gadgil 2003; Moron et al. 2017).

Incoherent fluctuations, extreme flood or deficient rainfall events, and high impact rainfall events often cause severe

damage and property loss in the Indian subcontinent during the monsoon season. The Indian monsoon rainfall is mainly affected/dominated by orography in the Western Ghats region and Himalayan area of North and North East of India.

The high impact rainfall events are often localized and associated with large-scale meteorological systems, for instance, depressions and cyclones. Policymakers and disaster managers are usually interested in future outlooks of such

extreme rainfall events from several monsoon season vagaries. In the context of climate change, where it is projected that extreme rainfall events are increasing during the monsoon season, the downscaling assumes a significant area of active research.

Meteorological forecasts and observations are often generated at a very coarse spatial resolution. While technology is available to perform dynamic forecasts at high spatial resolutions, it can be very compute-intensive and relatively expensive to manage the operational runs for such high spatial resolutions.

The generation of low-resolution climate forecasts (e.g., Swapna et al. (2018), Krishnan et al. (2019)) can be downscaled (von Storch et al. 1993; Wilby and Dawson 2013) for better regional outlook generation.

Similarly, downscaling of observed precipitation data can also be made based on a low-resolution observation (Sahai et al. 2017). Most landscape characteristics such as rivers, water systems, and utilities have much smaller dimensions than 100–500 km. Climate patterns, such as convective clouds and coastal breezes, could be captured after appropriate downscaling.

Downscaling requires a variety of approaches, each with its benefits and drawbacks. Several methods are available for downscaling meteorological information. They can be broadly classified as dynamical and statistical downscaling focusing on regional climate simulations (Kaur et al. 2020; Nobre et al. 2001; Díez et al. 2005; Shukla and Lettenmaier 2013; Xue et al. 2014). The statistical downscaling methods (von Storch et al. 1993; Zorita and von Storch 1999; Wilby and Dawson 2013; Sahai et al. 2017) have been applied in several studies mainly focusing on the downscaling of precipitation (von Storch et al. 1993; Vrac and Naveau 2007; Benestad 2010; Sahai et al. 2017).

Dynamical downscaling involves using the initial and boundary conditions from a global model and then running a high-resolution regional model to generate a local forecast. For example, city-level forecasts, which are often computationally expensive and time-consuming, require high-performance compute resources (Benestad and Haugen 2007; Benestad 2010; Kaur et al. 2020). On the other hand, statistical downscaling uses the outputs from the global dynamical models or observations as inputs to statistical models (ranging from simple univariate to complex multivariate schemes) to generate high-resolution (e.g., city-scale) information.

Statistical downscaling of rainfall (observation or forecast) is a popular (computationally) low-cost method (so-called the poor man's approach) to improve the rainfall information on regional scales and is made available to stakeholders and decision-makers (Salvi et al. 2013; Vandal et al. 2017). The world has moved towards artificial intelligence (AI) and machine learning (ML) techniques for statistical downscaling. Several studies show that AI-based downscaling methods could be suitable for

rainfall downscaling, which are often very non-linear and include multi-scale stochastic noise. Tripathi2006 has shown the strength of the support vector machine (SVM) method in the downscaling of precipitation data. The recent developments in single image super-resolution (SR) using deep learning (Dong et al. 2015) offer a promising hope in downscaling weather model outputs to high resolution. Figure 1c depicts a visual representation of the downscaling principle. This paper introduces a deep learning–based method for precipitation downscaling to generate high-resolution precipitation data over the Indian region during the summer monsoon (June–September) season, which can provide local projections. The next section of this paper describes methods followed by the results obtained in Section 3. Conclusion and discussion are provided in Section 4.

## 2 Methods

This study uses super-resolution-based convolutional neural networks (CNN), known as the SRCNN method, following Vandal et al. (2017, 2019). A low-resolution input image is used to map accurately to a high-resolution image in this method. SRCNN allows end-to-end mapping to be optimized and is faster than other super-resolution (SR) methods. It uses a low-resolution image in the first step, upgraded to the higher resolution size by using bicubic interpolation. Suppose the interpolated image is referred to as  $Y$ ; SRCNNs' task is to retrieve from  $Y$  an image  $F(Y)$  which is close to the high-resolution ground truth image  $X$ . We still call  $Y$  as a “low-resolution” image as the pixel level information is inaccurate in  $Y$  relative to  $X$ . Dong et al. (2015) showed that CNNs could accurately extract patches, conduct non-linear mapping, and reconstruct a low-resolution input to a high-resolution image.

Traditional SR approaches are used to boost the resolution of a factor of 2–4; statistical downscaling demands a conservative resolution increase of 8–12 factors. Similar to Vandal et al. (2019), we followed an alternative approach where instead of explicitly increasing the resolution to  $\times 8$ –12, it is achieved in many steps and known as stacked SRCNN.

We used stacked SRCNNs to boost the resolution to such a high degree that each SRCNN improves its resolution by one factor. The model can learn spatial pairs on multiple levels through this approach, requiring less complexity in the spatial representations. The ability to arbitrarily improve image resolutions from the lower resolution enables input/output pairs to train stacked SRCNNs on several scales. However, since the SRCNN output is again the SRCNN input, an unwanted network error may be distributed over the stacked layers when training a case by case model.

In general, one only requires a low-resolution (LR) image to approximate a high-resolution (HR) image while using an SR on pictures. Nonetheless, during statistical downscaling (SD), high-resolution data may be used to estimate the HR

images, which coincide with this LR image. For example, we can use two types of inputs for precipitation downscaling, such as maps of LR rainfall and static topographical features. Since topographical characteristics are defined in very high resolution and do not usually change over time, they can be used for any scaling factor. The method which uses topographies as an additional input to stacked SRCNN has been called the “DeepSD” by Vandal et al. (2019). A sketch in Fig. 2 provides an overview of SRCNN and DeepSD methods. Table 1 provides the data training parameters used in this work.

### 3 Data

In this work, we have primarily used rainfall data obtained from several sources. The theory is first developed using the daily IMD (Indian Meteorological Department) gridded data.

**Table 1** Square of correlation coefficient ( $r^2$ , %) of AI/ML models with IMD ground truth PC

| AI model name    | Mode 1 | Mode 2 | Mode 3 |
|------------------|--------|--------|--------|
| DeepSD, IMD      | 92     | 88     | 59     |
| Stack SRCNN, IMD | 92     | 88     | 67     |
| SRCNN, IMD       | 92     | 88     | 65     |

It may be seen that up to mode 2, all the models capture the temporal variability (represented by the CC of the PCs). However, as we go to the higher modes, the temporal variability is not faithfully represented. One of EOF-based modes’ drawbacks is that higher modes may lack physical relevance with the more geometrical modes. Hence, MSE and pattern CC-based PDF would be useful to represent the variability of total fields. Thus, based on these two metrics, we can infer that the downscaled AI/ML models captured the large-scale patterns and the model preserves the temporal variability of the ground truth data.

Data on two spatial resolutions are used. The low-resolution  $1^\circ \times 1^\circ$  spatial resolution data is used as input to the AI/ML

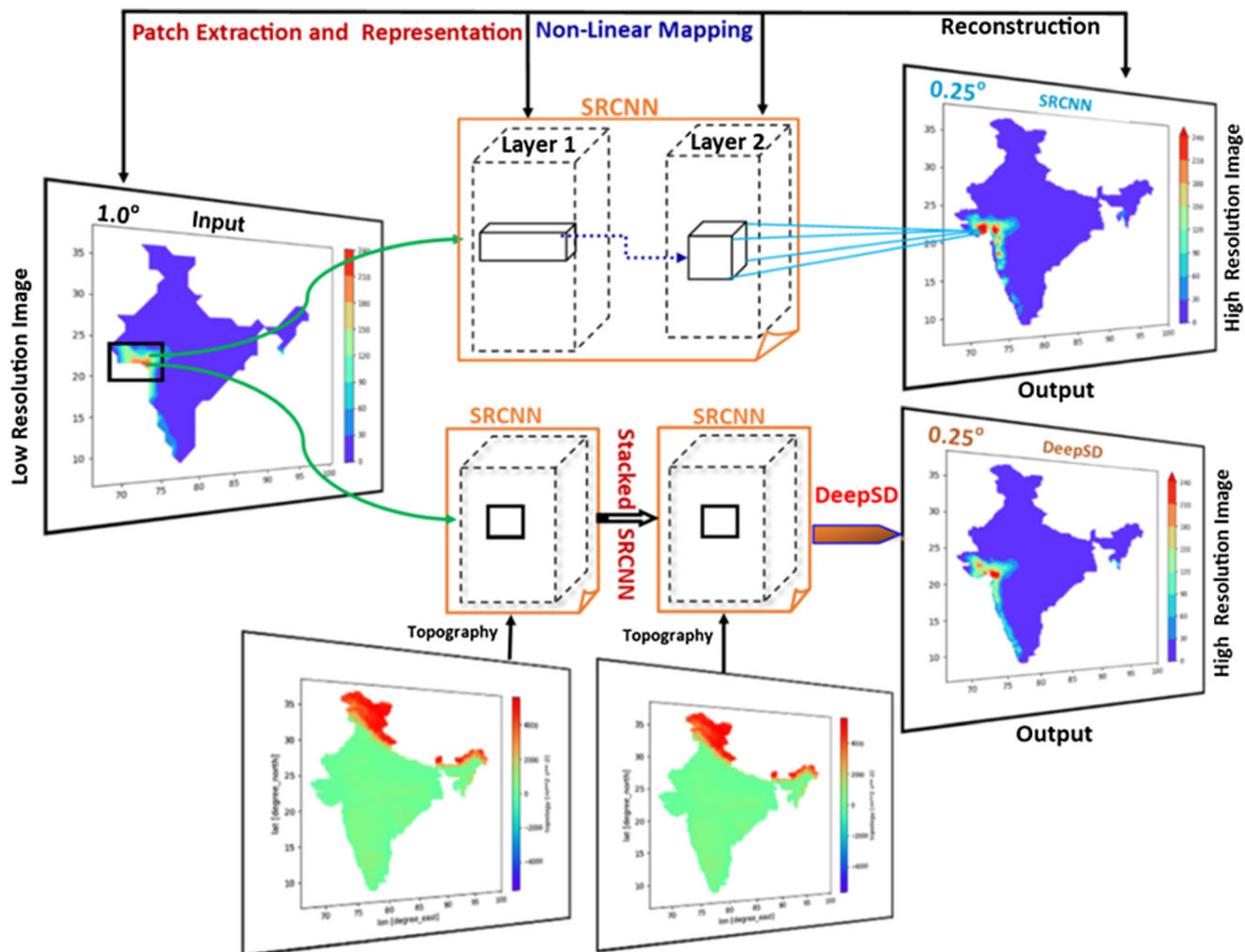


**Fig. 2** An overview of SRCNN and DeepSD methods. In the DeepSD, the downscaling is done in steps rather than a direct  $\times 4$  or  $\times 8$  resolution. Also, DeepSD used multivariable inputs



network, and the  $0.25^\circ \times 0.25^\circ$  is used for verification (ground truth) data. The low-resolution ( $1^\circ \times 1^\circ$ ) data is generated from the high-resolution data using linear interpolation. The IMD data is prepared from the Indian land station data described in Rajeevan et al. (2006, 2008) and Pai et al. (2014). For each day, the  $1^\circ$  data has the latitude  $\times$  longitude dimension of  $33 \times 35$ , and  $0.25^\circ$  data has the latitude  $\times$  longitude dimension of  $129 \times 135$ . Apart from the IMD daily gridded data, the TRMM data (Huffman et al. 2007) of resolutions ( $0.25^\circ \times 0.25^\circ$ ) was also used to test these algorithms. We have also used the fifth generation of ECMWF atmospheric reanalysis of the global climate (ERA5) rainfall data (Hersbach et al. 2020). This data was downloaded from the Copernicus Climate Data Server (CDS) to demonstrate the potential application of the AI/ML-based method for the post-processing (i.e., downscaling and bias-correction) of reanalysis rainfall data as a potential application of the concept developed using IMD data over the Indian region.

### 3.1 Data pre-processing

Original data obtained from IMD has values only on the land surface area. However, for applying the CNN algorithm, the square/rectangular shape data is required for 2D convolution. The 2D convolution kernels are generally square and are applied to the whole matrix. The original data had a triangular shape, based on the data availability over the Indian region. The missing values over the Ocean and landmass are filled with significantly large negative values in the IMD gridded dataset. First of all, negative values outside Indian region limits were converted into “NaN.” Then additional “NaN” values were padded to make matrix size of  $140 \times 140$  from  $129 \times 135$  originally, as shown in Fig. 4. A similar transformation is used to make the square shape for TRMM data and ERA5 rainfall data.

### 3.2 Training and testing

Three methods described in the previous section (Section 2) were employed on the IMD data to develop a model for creating high-resolution data. The training was done for 30 years on the  $1^\circ \times 1^\circ$  IMD data, i.e., from the year 1975 to 2004 for the June to September period. A systematic analysis was carried out to select the best data training architecture for each model. The developed models were tested on 5 years of the monsoon season data (122 days of June–September) from 2005 to 2009. The resulted outputs were compared with ground truth, i.e.,  $0.25^\circ$  IMD gridded data. Similarly, the TRMM and ERA rainfall data is also partitioned as training and test period data.

### 3.3 Verification metrics

In this study, we use two types of verification metrics. The first metric is the traditional mean square error (MSE) and pattern correlation coefficient (cc)–based approach, and the second metric is based on the multivariate statistical analysis approach. The fidelity of the AI/ML model output data is first tested for the Indian region by plotting the probability density function (PDF) of *cc* and *MSE* computed for all the grid points where data is available or undefined. The *cc* and *MSE* for each grid point are computed based on the 5 years  $\times$  122 days = 610 days of data. PDFs of *cc* and *MSE* are plotted for the grid points where the metric is computable (i.e., a grid point out of the total  $129 \times 135 = 17415$  grid points which do not have undefined or NaN attribute for all the 610 days). In the next step, we have calculated the principal components (*pc*) and the Eigenvectors of the covariance matrix (i.e., empirical orthogonal functions, aka *EOF*) (Hersbach et al. 2020) for the spatial data over the Indian region. The first three *pcs* and *EOFs* are plotted to see that the principal components’ dominant spatial variance and the temporal evolutions are faithfully represented by outputs from the AI/ML-based networks.

## 4 Results and discussion

The models developed have been employed to two different sets of data, as mentioned in Section 2. Here, we provide details of the analysis done on these data.

### 4.1 Downscaling of IMD data

For visual comparison, 2D images of rainfall amount on a particular day in a year were compared, as shown in Fig. 3. These days are a representative of heavy precipitation on the east coast and west coast monsoon rainfall.

In Fig. 3, the rainfall amount obtained from three methods, viz., SRCNN, stacked SRCNN, and DeepSD, are compared with ground truth and traditional linear interpolation. Panel (b) is the original input having resolution  $1^\circ$ , and panels (a) and (c) represent the linear interpolation to  $0.25^\circ$  and ground truth of  $0.25^\circ$  resolution, respectively. Outputs obtained from the three methods are represented by panels (d), (e), and (f), which are to be compared with panels (a) and (c). Rectangles indicate the prime region of maximum rain in the southwestern part of India. The results obtained from all three methods captured better rainfall than the traditional linear interpolation method (panel a). This comparison of findings suggests that DeepSD is a better tool for downscaling.

Similar comparisons were also made for extreme case years which are drought year and extra monsoon year. In those comparisons (not shown here) too, DeepSD was found to be the best method. However, it does not sound right to draw

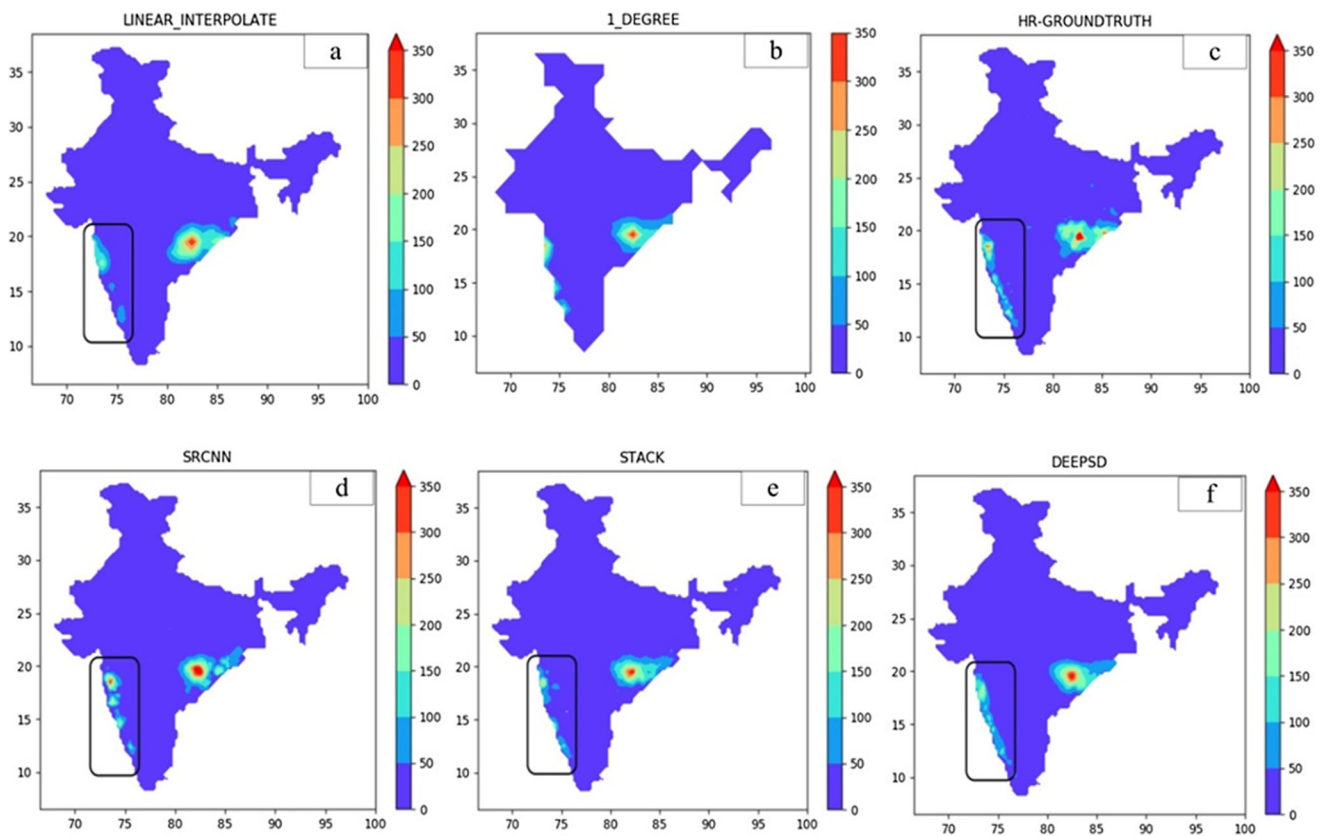


**Fig. 3** Comparison of downscaling output resulted from three AI models applied in this study with traditional linear interpolation. The data is for the year 2006 and day 183. The rainfall amounts shown are in millimeters (mm) per day

generalized conclusions based on these few comparisons. Therefore, we have carried out a statistical analysis and compared two measures: pattern correlation (CC) and mean square error (MSE in  $\text{mm}^2/\text{day}$ ) for the three methods with PDF plotted in Fig. 4 as discussed in Section 3.3.

In this comparison also, the DeepSD model was found to be better among the three methods as it shows the highest frequency (probability density) of maximum correlation value and the lowest MSE peak frequency, as seen in the Fig. 4. Interestingly, using this metric, we find that all these methods have performed better than conventional linear interpolation (blue curve).

Furthermore, as another test, the entire data was divided into four quartiles based on the count of grid points where rainfall values are more than 30 mm. Model results were compared in the upper quartile and also ensure that they are consistent. Figure 5 contains comparisons for PDFs of pattern correlation as well as MSE. Similar to results for entire data, here also the DeepSD stood as the best method among all three.

In order to see if the AI/ML-based downscaled data has preserved the spatial coherence and the dominant mode of variability is represented adequately, we plotted the first three EOFs of the downscaled data together with ground truth,

**Fig. 4** Comparisons of correlation PDF and MSE ( $\text{mm}/\text{day}$ )<sup>2</sup> using three methods applied on IMD data

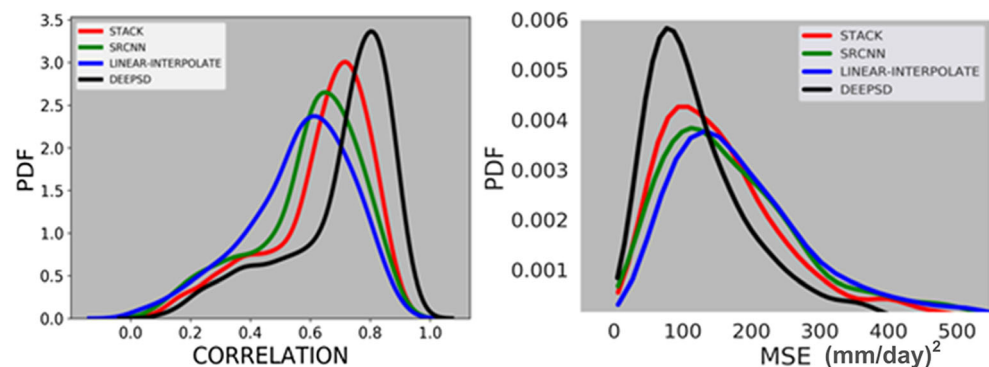
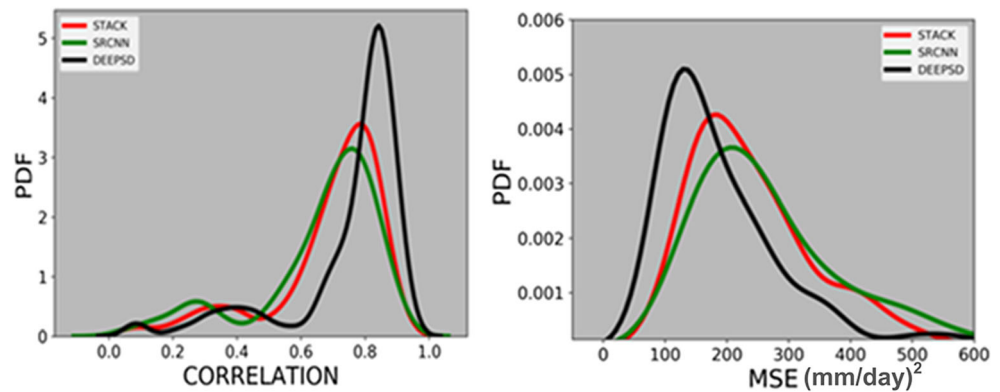


**Fig. 5** Comparisons of correlation PDF and MSE ( $\text{mm/day}$ )<sup>2</sup> using three methods on upper quartile only



which are depicted in Fig. 6. It can be seen that the dominant modes of all the methods represent the dominant spatial covariance pattern for the observation, although the first three modes overestimated the spatial variance (mentioned at the top right of each panel). The  $r^2$  (square of correlation) values of the pcs are shown in Table 1.

## 4.2 Downscaling of TRMM data

The application of the above three methods on IMD data assured that “DeepSD” is the best method for downscaling. This method was applied to TRMM data to downscale from  $0.5^\circ$  to  $0.25^\circ$  resolution to re-confirm this analysis.

The total data used in the case was 17 years, i.e., 1998–2015, out of which 15 years of the data were used for model training and the rest of the years (2014–2015) for model validation. Details of parameters used for training and testing this data are the same as those in Table 1. Results were then compared with traditional linear interpolation.

The correlation and MSE PDFs were computed and compared with linear interpolation. It was found that DeepSD has a better correlation and less MSE than the linear interpolation shown in Fig. 7.

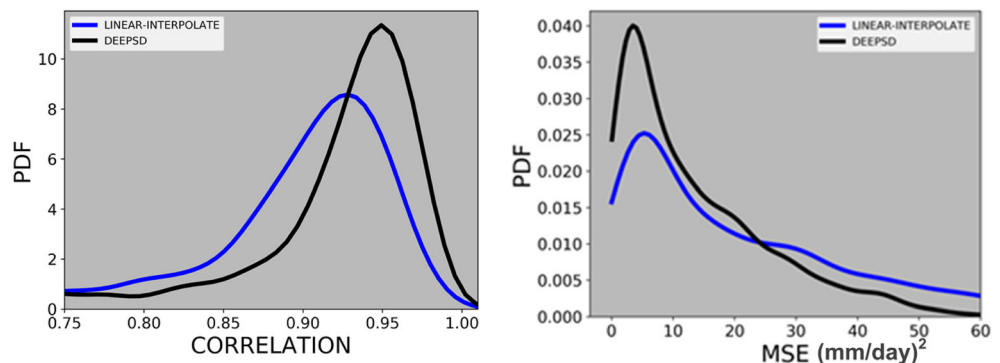
## 4.3 Application for model data post-processing

### 4.3.1 Model data post-processing

We have applied this model for the post-processing of ERA5 reanalysis data. In this case, the model’s training was done using ERA5 data and IMD gridded data as ground truth. The training data was 25 years, in particular, from 1979 to 2004. The testing was done on the JJAS period from 2005 to 2009. Similar to IMD and TRMM data, in this case, DeepSD was found to be better than SRCNN. A comparison of correlation and MSE using original ERA5 data, SRCNN, and DeepSD is shown in Fig. 8.

Similar to the IMD rainfall post-processing, we also use the EOF-based metric to evaluate the dominant mode of variability’s spatial patterns. Figure 9 shows that compared to the raw ERA5 rainfall, the variance distribution of ERA5 rainfall post-processed using AI/ML methods is better. In particular, variances across northern India, north-west India, and Kashmir have been better captured with AI/ML-based post-processing methods. Also, the  $r^2$  (square of the correlation coefficient) improves a lot (see Table 2) in the AI/ML-based post-processed data compared to the raw ERA5 data.

**Fig. 6** Comparison of correlation and MSE ( $\text{mm/day}$ )<sup>2</sup> PDF for TRMM data. Correlation calculated from the DeepSD method is better than the linear interpolation. MSE is slightly less in the case of DeepSD than the linear interpolation



## EOF of Rainfall JJAS 2005-2009

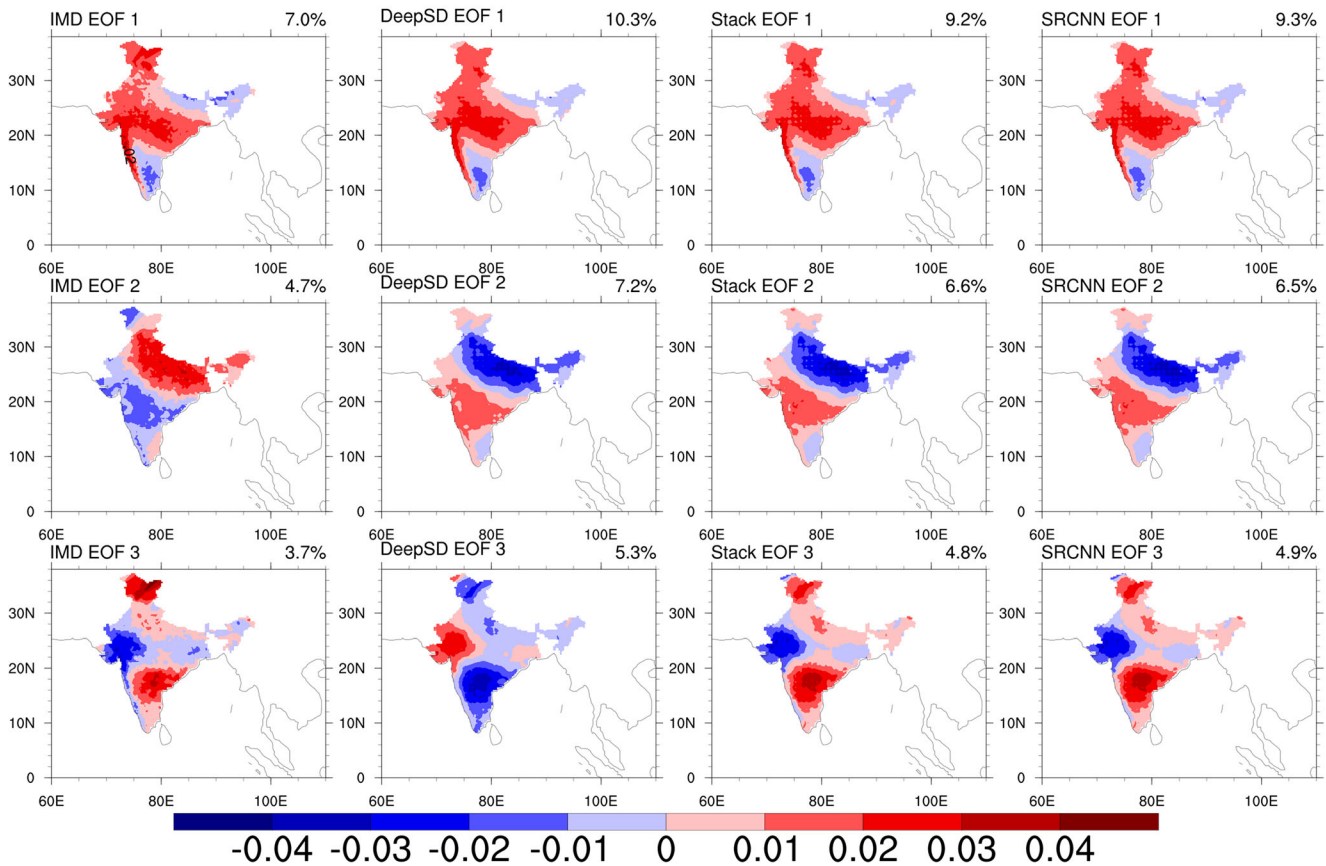


**Fig. 7** First three empirical orthogonal functions (EOFs) of IMD ground truth data (1st column panels) and AI/ML-based models are mentioned at the top of each model (2nd column is for DeepSD, 3rd for stacked

SRCNN, and last depicts SRCNN EOFs). The variance explained by each mode is also mentioned at the top right of each panel. The amplitudes of shading are arbitrary units

### 4.3.2 Scale-free downscaling

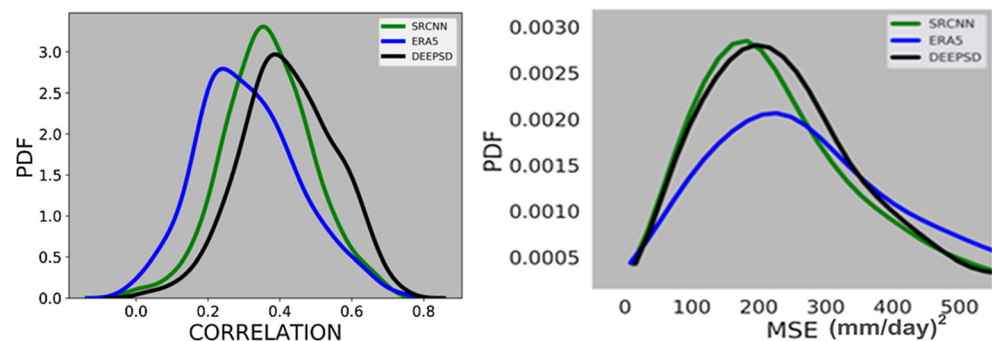
These results proved that DeepSD is the best method among the three methods discussed in this work. Based on our experience in  $1 \times 1$  to  $0.25 \times 0.25$  degree downscaling, we hypothesize that SRCNN or DeepSD-based method will provide the realistic amplitude and intensity of extreme events without any loss of information. We applied this model to generate  $0.125^\circ$  data using  $0.25^\circ$  data obtained from IMD observation.

A comparison of the resulted high-resolution map obtained from traditional linear interpolation and our models, namely, SRCNN and DeepSD, is shown in Fig. 10.

## 5 Conclusion

This study has employed an application based on AI/ML-based techniques, namely, SRCNN and DeepSD, to

**Fig. 8** Comparison of correlation and MSE  $(\text{mm/day})^2$  PDF for TRMM Data. The blue color line is for original ERA5 data





## EOF of Rainfall JJAS 2005–2009

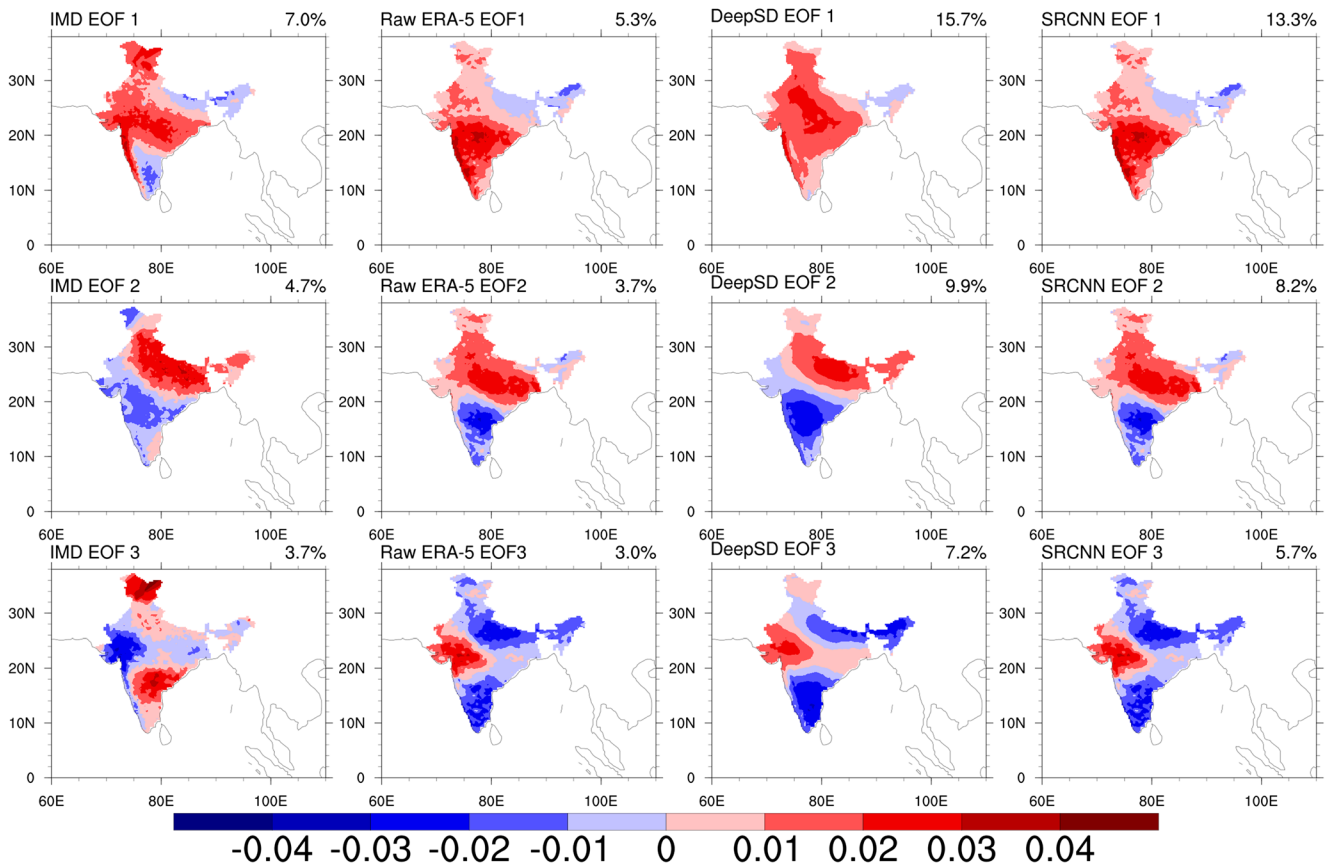


**Fig. 9** The first row (3 panels from top to bottom) represents the EOFs for IMD ground truth; 2nd row shows the raw ERA-5 reanalysis rainfall data. The EOFs for AI/ML-based post-processed data using the ERA-5 reanalysis data as input (mentioned at the top of each panel) are shown in the 3rd

and 4th rows. The variance explained by each of the modes is also mentioned at the top right of each panel. The amplitudes of shading are arbitrary units

downscale the Indian region's rainfall information. The analysis shows that the DeepSD-based method has a better correlation and lowest MSE than the conventional linear interpolation approaches. The AI/ML-based approach provides better information on rainfall intensity as compared to linear interpolations. It is well known that the AI/ML-based method has the advantage of superior gradient or edge detection than linear techniques.

**Table 2** Square of correlation coefficient ( $r^2$ , %) between AI/ML-based ERA5 post-processed rainfall and IMD rainfall

|                  | Mode 1 | Mode 2 | Mode 3 |
|------------------|--------|--------|--------|
| Raw-ERA5, IMD    | 58     | 43     | 18     |
| DeepSD-ERA5, IMD | 67     | 68     | 18     |
| SRCNN-ER5, OBS   | 68     | 59     | 14     |

The downscaling of precipitation based on this hypothesis of superior edge detection by AI/ML-based methods could improve the spatial distribution of downscaled rainfall. This hypothesis has been verified for rainfall data, and the benefits of AI/ML-based downscaling have been demonstrated.

It is shown that the spatial discontinuity in amplitude and intensity rainfall patterns is the main obstacle in the downscaling of precipitation over the Indian region. The AI/ML method applied to the station derived meteorological data (IMD) has the advantage of preserving this spatial discontinuity of rainfall data without any loss in intensity. The model has been used on two different data types, namely, IMD gridded data obtained from the ground (station) observation and the satellite-derived TRMM data. In both cases, the best correlations were found with “DeepSD,” and the lowest MSE was obtained using this method.

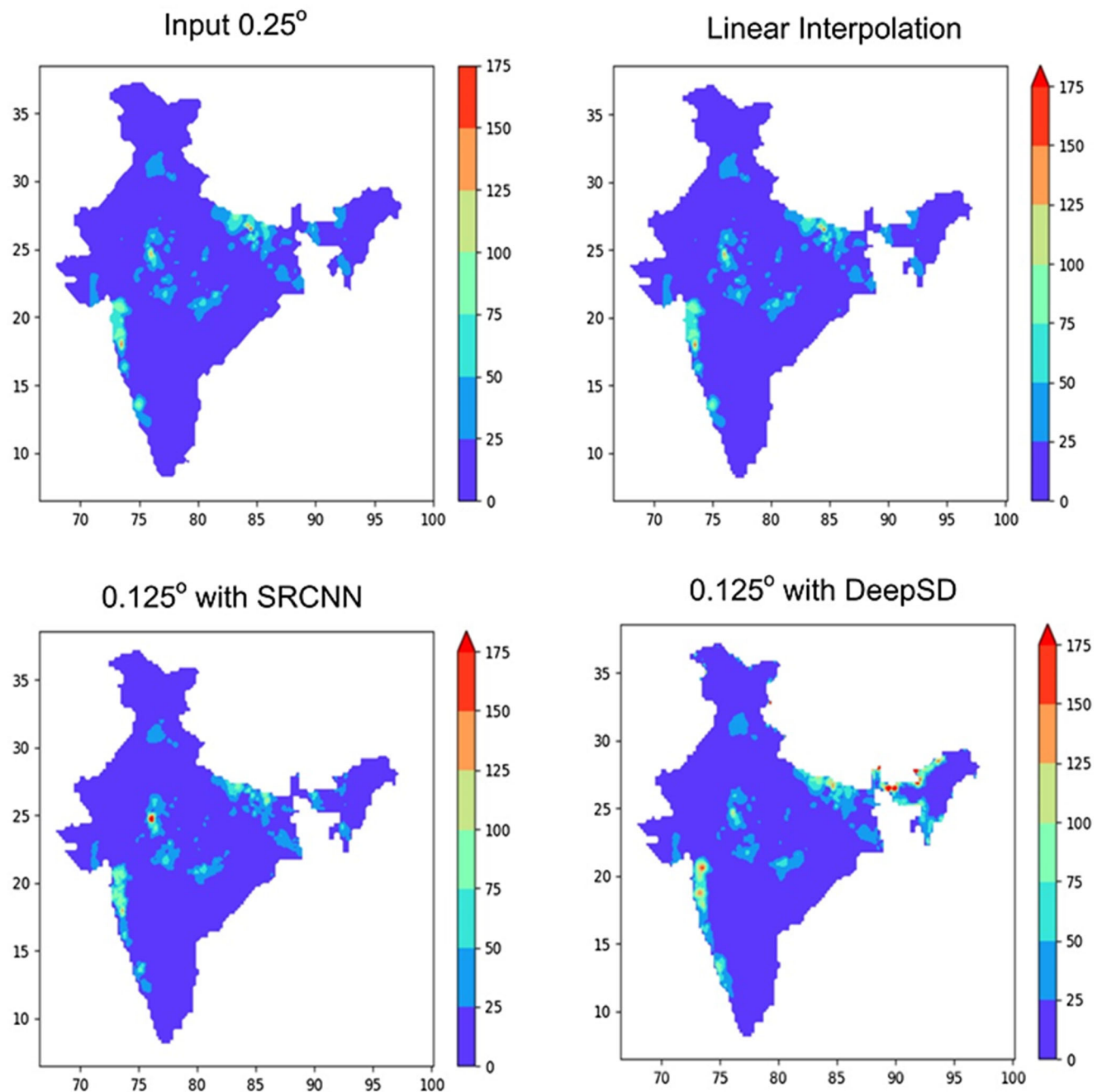


**Fig. 10** Application of developed models. A high-resolution ( $0.125^\circ \times 0.125^\circ$ ) rainfall map over the Indian region (landmass) was generated using SRCNN and DeepSD methods. The map resulted from the DeepSD

shows better rainfall intensity. Since no such high-resolution observation data is available at IMD, it cannot be validated with observation

Similarly, it is found that the AI/ML-based model can be used in a proficient manner to bias correct the reanalysis rainfall. The post-processed ERA5 rainfall data using the AI/ML techniques show much better distribution of spatial covariance and the temporal variance when compared with observation. Thus, the AI/ML-based post-processing and downscaling is proposed to be an efficient and skillful method for rainfall data over the Indian region.

After validating these methods, we have generated very high-resolution ( $0.125^\circ \times 0.125^\circ$ ) rainfall maps over the Indian region using input data of  $0.25^\circ \times 0.25^\circ$  resolution. This work can be the first step towards developing deep learning-based meteorological data downscaling models.

**Acknowledgment** IITM is funded by the Ministry of Earth Sciences, Government of India. The authors would like to thank Dr. David John

Gagne, NCAR, for a constructive discussion and suggestions on this manuscript.

**Authors' contributions** Concept and design: B.K., R.C., and M.S. conceptualize the idea of problem statement and finalized the algorithms for methods used in this study.

Drafting of manuscript: B.K. and R.C. mainly contributed in manuscript writing. M.S. also helped to finalize the text for manuscript.

Code development: N.C. and K.D. developed the code. M.S. and A.B. supervised the code development and plotting of figures.

Acquisition of data: R.C. and M.S. contributed in data collection and pre-processing.

Critical revision: R.C. and M.S. did the critical revision of the manuscript.

**Funding** This work is a part of a student project completed at IITM. No additional funding support was received. This work was done on the HPC facility provided by the Ministry of Earth Sciences at IITM Pune.

**Data availability** The details of HPC can be found on [prtyush.tropmet.res.in](http://prtyush.tropmet.res.in). IMD rainfall data is obtained from India Meteorological Department, Pune. The TRMM data is available at [https://disc.gsfc.nasa.gov/datasets/TRMM\\_3B42\\_Daily\\_7/summary](https://disc.gsfc.nasa.gov/datasets/TRMM_3B42_Daily_7/summary). The ERA5 rainfall data is downloaded from <https://cds.climate.copernicus.eu/>.

## Compliance with ethical standards

**Conflict of interest** The authors declare that they have no conflict of interest.

## References

- Ashok K, Guan Z, Yamagata T (2001) Impact of the Indian Ocean dipole on the relationship between the Indian monsoon rainfall and ENSO. *Geophys Res Lett* 28:4499–4502. <https://doi.org/10.1029/2001GL013294>
- Benestad RE (2010) Downscaling precipitation extremes. *Theor Appl Climatol* 100:1–21. <https://doi.org/10.1007/s00704-009-0158-1>
- Benestad RE, Haugen JE (2007) On complex extremes: flood hazards and combined high spring-time precipitation and temperature in Norway. *Clim Chang* 85:381–406. <https://doi.org/10.1007/s10584-007-9263-2>
- Chang C-P, Johnson RH, Ha K-J, Kim D, Ngar-Cheung Lau G, Wang B, Bell MM, Luo Y (2018) The multiscale global monsoon system: research and prediction challenges in weather and climate. *Bull Am Meteorol Soc* 99:ES149–ES153. <https://doi.org/10.1175/BAMS-D-18-0085.1>
- Diez E, Primo C, García-moya JA, Gutiérrez JM, Orfila B (2005) Statistical and dynamical downscaling of precipitation over Spain from DEMETER seasonal forecasts. *Tellus A* 57:409–423. <https://doi.org/10.1111/j.1600-0870.2005.00130.x>
- Dong, C, Chen, Loy CC, He K, Tang X (2015) Image super-resolution using deep convolutional networks. *CoRR* abs/1501.00092:
- Gadgil S (2003) The Indian monsoon and its variability. *Annu Rev Earth Planet Sci* 31:429–467. <https://doi.org/10.1146/annurev.earth.31.100901.141251>
- Gadgil S, Yadumani, Joshi NV (1993) Coherent rainfall zones of the Indian region. *R Meteorol Soc* 13:546–566. <https://doi.org/10.1002/joc.3370130506>
- Hersbach H, Bell B, Berrisford P, Hirahara S, Horányi A, Muñoz-Sabater J, Nicolas J, Peubey C, Radu R, Schepers D, Simmons A, Soci C, Abdalla S, Abellan X, Balsamo G, Bechtold P, Biavati G, Bidlot J, Bonavita M, Chiara G, Dahlgren P, Dee D, Diamantakis M, Dragani R, Flemming J, Forbes R, Fuentes M, Geer A, Haimberger L, Healy S, Hogan RJ, Hólm E, Janisková M, Keeley S, Laloyaux P, Lopez P, Lupu C, Radnoti G, Rosnay P, Rozum I, Vamborg F, Villaume S, Thépaut JN (2020) The ERA5 global reanalysis. *Q J R Meteorol Soc* 146:1999–2049. <https://doi.org/10.1002/qj.3803>
- Huffman GJ, Bolvin DT, Nelkin EJ, Wolff DB, Adler RF, Gu G, Hong Y, Bowman KP, Stocker EF (2007) The TRMM multisatellite precipitation analysis (TMPA): quasi-global, multiyear, combined-sensor precipitation estimates at fine scales. *J Hydrometeorol* 8:38–55. <https://doi.org/10.1175/JHM560.1>
- Kaur M, Krishna RPM, Joseph S, Dey A, Mandal R, Chattopadhyay R, Sahai AK, Mukhopadhyay P, Abhilash S (2020) Dynamical downscaling of a multimodel ensemble prediction system: application to tropical cyclones. *Atmos Sci Lett* 21:e971. <https://doi.org/10.1002/asl.971>
- Krishnan R, Sugi M (2003) Pacific decadal oscillation and variability of the Indian summer monsoon rainfall. *Clim Dyn* 21:233–242. <https://doi.org/10.1007/s00382-003-0330-8>
- Krishnan R, Swapna P, Vellore R, et al (2019) The IITM earth system model (ESM): development and future roadmap. In: *Current Trends in the Representation of Physical Processes in Weather and Climate Models*. In: The IITM Earth System Model (ESM): Development and Future Roadmap. Springer Singapore, pp 183–195
- Moron V, Robertson AW, Pai DS (2017) On the spatial coherence of sub-seasonal to seasonal Indian rainfall anomalies. *Clim Dyn* 49:3403–3423. <https://doi.org/10.1007/s00382-017-3520-5>
- Nobre P, Moura AD, Sun L (2001) Dynamical downscaling of seasonal climate prediction over Nordeste Brazil with ECHAM3 and NCEP's regional spectral models at IRI. *Bull Am Meteorol Soc* 82(12): 2787–2796. Retrieved Dec 4, 2020, from [https://journals.ametsoc.org/view/journals/bams/82/12/1520-0477\\_2001\\_082\\_2787\\_ddosep\\_2\\_3\\_co\\_2.xml](https://journals.ametsoc.org/view/journals/bams/82/12/1520-0477_2001_082_2787_ddosep_2_3_co_2.xml)
- Pai DS, Sridhar L, Rajeevan M et al (2014) Development of a new high spatial resolution ( $0.25^\circ \times 0.25^\circ$ ) long period (1901–2010) daily gridded rainfall data set over India and its comparison with existing data sets over the region. *Mausam Indian Meteorol Dep* 65:1–18
- Pant GB, Parthasarathy SB (1981) Some aspects of an association between the southern oscillation and Indian summer monsoon. *Arch Meteorol Geophys Bioclimatol Ser B* 29:245–252. <https://doi.org/10.1007/BF02263246>
- Rajeevan M, Bhate J, Jaswal AK (2008) Analysis of variability and trends of extreme rainfall events over India using 104 years of gridded daily rainfall data. *Geophys Res Lett* 35. <https://doi.org/10.1029/2008GL035143>
- Rajeevan M, Bhate J, Kale JD, Lal B (2006) High resolution daily gridded rainfall data for the Indian region: analysis of break and active monsoon spells. *Curr Sci Assoc* 91:296–306
- Sahai AK, Borah N, Chattopadhyay R, Joseph S, Abhilash S (2017) A bias-correction and downscaling technique for operational extended range forecasts based on self organizing map. *Clim Dyn* 48:2437–2451. <https://doi.org/10.1007/s00382-016-3214-4>
- Salvi K, Kannan S, Ghosh S (2013) High-resolution multisite daily rainfall projections in India with statistical downscaling for climate change impacts assessment. *J Geophys Res Atmos* 118:3557–3578. <https://doi.org/10.1002/jgrd.50280>
- Shukla S, Lettenmaier DP (2013) Multi-RCM ensemble downscaling of NCEP CFS winter season forecasts: implications for seasonal hydrologic forecast skill. *J Geophys Res Atmos* 118:10,770–10,790. <https://doi.org/10.1002/jgrd.50628>
- Sikka DR (1980) Some aspects of the large scale fluctuations of summer monsoon rainfall over India in relation to fluctuations in the planetary and regional scale circulation parameters. *Proc Indian Acad Sci - Earth Planet Sci* 89:179–195. <https://doi.org/10.1007/BF02913749>

- Singh M, Krishnan R, Goswami B et al (2020) Fingerprint of volcanic forcing on the ENSO–Indian monsoon coupling. *Sci Adv* 6: eaba8164. <https://doi.org/10.1126/sciadv.aba8164>
- Swapna P, Krishnan R, Sandeep N, Prajeesh AG, Ayantika DC, Manmeet S, Vellore R (2018) Long-term climate simulations using the IITM earth system model (IITM-ESMv2) with focus on the South Asian monsoon. *J Adv Model Earth Syst* 10:1127–1149. <https://doi.org/10.1029/2017MS001262>
- Vandal T, Kodra E, Ganguly AR (2019) Intercomparison of machine learning methods for statistical downscaling: the case of daily and extreme precipitation. *Theor Appl Climatol* 137:557–570. <https://doi.org/10.1007/s00704-018-2613-3>
- Vandal T, Kodra E, Ganguly S, et al (2017) DeepSD: generating high resolution climate change projections through single image super-resolution. *arXiv.org* 1–9. <https://arxiv.org/abs/1703.03126>
- von Storch H, Zorita E, Cubasch U (1993) Downscaling of global climate change estimates to regional scales: an application to Iberian rainfall in wintertime. *J Clim* 6:1161–1171. [https://doi.org/10.1175/1520-0442\(1993\)006<1161:DOGCCE>2.0.CO;2](https://doi.org/10.1175/1520-0442(1993)006<1161:DOGCCE>2.0.CO;2)
- Vrac M, Naveau P (2007) Stochastic downscaling of precipitation: from dry events to heavy rainfalls. *Water Resour Res* 43. <https://doi.org/10.1029/2006WR005308>
- Wilby RL, Dawson CW (2013) The Statistical DownScaling Model: insights from one decade of application. *Int J Climatol* 33:1707–1719. <https://doi.org/10.1002/joc.3544>
- Xue YK, Janjic Z, Dudhia J, Vasic R, De Sales F (2014) A review on regional dynamical downscaling in intraseasonal to seasonal simulation/prediction and major factors that affect downscaling ability. *Atmos Res* 147:68–85. <https://doi.org/10.1016/j.atmosres.2014.05.001>
- Zorita E, von Storch H (1999) The analog method as a simple statistical downscaling technique: comparison with more complicated methods. *J Clim* 12:2474–2489. [https://doi.org/10.1175/1520-0442\(1999\)012<2474:TAMAAS>2.0.CO;2](https://doi.org/10.1175/1520-0442(1999)012<2474:TAMAAS>2.0.CO;2)

**Publisher's note** Springer Nature remains neutral with regard to jurisdictional claims in published maps and institutional affiliations.